



## Study of channel divergence on the flow and heat transfer in horizontal ducts heated from a side

C.S. Yang<sup>a</sup>, C.G. Liu<sup>b,1</sup>, C. Gau<sup>b,\*</sup>

<sup>a</sup> Department of Computer Science and Information Engineering, Far East University, Taiwan

<sup>b</sup> Institute of Aeronautics and Astronautics and Center for Micro/Nano Science and Technology, National Cheng Kung University, Taiwan

Received 15 November 2007; received in revised form 24 January 2008; accepted 29 February 2008

Available online 1 April 2008

### Abstract

Experimental studies of convection flow and heat transfer in a horizontal divergent duct heated from a side which induces combined natural and forced convection have been carried out. For the purpose of comparison, a duct made of two vertical parallel plates with one of the plates heated uniformly and the opposite plate well insulated is also made. The divergent duct is formed in a similar channel by inclining the insulated vertical wall with respect to the heated vertical wall so as to create a divergent angle of  $3^\circ$  with a larger exit. The gap between the plates is small and the height to the gap ratio of the channel cross section is 6.67 at the entrance. Both flow visualization and the heat transfer along the heated wall are measured. The Reynolds number ranges from 316 to 1500, the buoyancy parameter,  $Gr/Re^2$  from 0 to 20000 and  $Pr$  of the airflow is 0.707. The effect of the Reynolds number and the buoyancy parameter on the heat transfer is presented and discussed. It is found that the small divergence of the duct can have a significant effect on both the flow and the local heat transfer. However, enhancement of the heat transfer can make the averaged Nusselt number approaches to the results of the parallel channel.

© 2008 Elsevier Masson SAS. All rights reserved.

**Keywords:** Mixed convection flow; Buoyancy effect; Horizontal channel; Heat transfer

### 1. Introduction

Mixed convection in channels has received great interest in the last three decades for its practical application in the solar energy collectors, heat exchangers, geothermal energy systems, chemical deposition of solid layer in the semiconductor industry, and the cooling of the nuclear reactors and modern electronic equipment. Most of the work in the past has been concerned with the mixed convection in a vertical parallel plate channel [1–4], or a horizontal parallel plate channel [5–9]. Review on the relevant work can be found in Ref. [10]. However, different orientations and heating conditions of the channel can induce different kinds of heated buoyant flows which enhance the heat transfer in different manners. For asymmetric heated vertical channel, when the buoyancy parameter is not large, the

small amount of the buoyant flow induced along the heated wall can either assist or oppose the main flow and cause either enhancement or reduction in the heat transfer. When the buoyancy parameter becomes large, the heated buoyant flow along the side wall becomes substantial. Depending upon the flow direction of the mainstream, the buoyant flow can cause different kinds of flow reversals which will change the entire flow characteristic and enhance the heat transfer in different manners. For horizontal channel, the heating is usually from the below [5–10]. Therefore, enhancement in the heat transfer can be obtained from the initiation of the secondary flow. This secondary flow is usually a heated buoyant flow which forms in mushroom shaped plumes associated with vortices. This kind of secondary flow is a laminar plume in the upstream and may become transformed into two-dimensional convection rolls, a very irregular flow or even a turbulent flow in the downstream region. The transition into different kind of flows depends on the magnitudes of the Reynolds number and the buoyancy parameter. Therefore, it appears that the mixed convection in a channel with different orientation and heating condition differs

\* Corresponding author.

E-mail address: [gauc@mail.ncku.edu.tw](mailto:gauc@mail.ncku.edu.tw) (C. Gau).

<sup>1</sup> Present address: Department of Aeronautics and Astronautics, Chinese Air Force Academy, Taiwan 83001, ROC.

## Nomenclature

$d$	channel gap (width)
$D_h$	hydrodynamic diameter, $2d$
$g$	gravitational acceleration
$Gr$	Grashof number, $g\beta q w^4 / k\nu^2$
$h$	transverse average in heat transfer coefficient
$h_l$	local heat transfer coefficient on the heated wall, $q/(T_w - T_o)$
$\bar{h}$	overall average in heat transfer coefficient
$k$	thermal conductivity of air
$Nu$	transverse average in the Nusselt number, $hD_h/k$
$Nu_l$	local Nusselt number, $h_l D_h/k$
$\bar{Nu}$	overall average in the Nusselt number, $\bar{h} D_h/k$
$Pr$	Prandtl number, $\nu/\alpha$
$q$	heat flux
$Re$	Reynolds number defined at the inlet of the channel, $u_o D_h/\nu$

$T$	temperature
$u_o$	inlet velocity
$w$	height of the channel
$x, y$	coordinate along the heated wall parallel, and normal to the streamwise direction

## Greek symbols

$\beta$	coefficient of thermal expansion
$\nu$	kinematic viscosity

## Subscript

$b$	refers to bulk mean
$f$	refers to pure forced convection
$nat$	refers to natural convection
$o$	refers to inlet
$w$	refers to heated wall

drastically, studies on the flow and heat transfer in a different channel must be carefully performed in a separated manner.

One of the current geometry of ducts is a horizontal rectangular channel formed by two 20 cm × 47 cm vertical parallel plate with one of the walls heated uniformly and the other well insulated. Work in this kind of configuration is very few [11]. Other recent work which may be relevant to the current study can be found in [12,13]. The gap between the plates is narrow and is 3 cm at the entrance. The current configuration of geometry has the potential application in the cooling of electronic equipments. When the circuit boards with electronic circuits printed in one side of the walls are arranged in parallel with passage in between for cooling air moving horizontally, one can have the current configuration of ducts. In addition, the current work also considers the situation when the insulated wall is inclined with respect to the heated vertical wall so that it creates a larger exit and a three degree angle of divergence with to the heated plate. This inclination is made to study whether a slight inclination of the vertical wall can have a significant effect on the flow and heat transfer as presented in other configurations [14–18]. The slight inclination of the vertical plate so as to create a convergent or a divergent channel may frequently be encountered in cooling of practical electronic equipments. It appears that the heat transfer data obtained before in the heated vertical channel or the horizontal channel heated from below could not be used in the current geometry. Work in this kind of channel or ducts and heating condition is not found in literature. Therefore, a systematic study on the mixed convection flow and the heat transfer is needed. Both flow visualization and the heat transfer measurements are preformed to gain a good understanding of the physical process and to provide some useful data.

## 2. Experimental apparatus and procedures

Experiments are performed in a plexiglas made parallel plate or divergent channel. The channel is connected with outlet of a

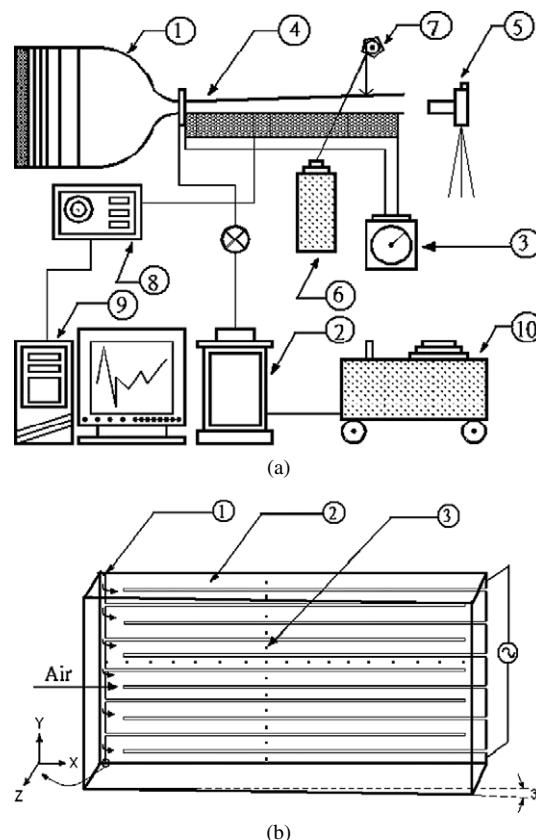


Fig. 1. Schematic diagram for (a) the experimental set up which include (1) wind tunnel, (2) smoke generator, (3) DC power supply, (4) Plexiglas channel, (5) camera, (6) laser, (7) rotating mirror, (8) data acquisition system, (9) personal computer and (10) compressor to blow smoke from smoke generator into the channel, and (b) the vertical divergent channel which include (1) slot for smoke injection, (2) stainless steel foil, and (3) 12 rows of thermocouples in the transverse direction.

wind tunnel system, as shown Fig. 1(a). The wind tunnel has a rectangular shape of contraction with dimensions of 20 cm × 3 cm. The vertical channel inside has an inlet dimension exactly

the same as the contract of the wind tunnel. The length of the channel is 47 cm. Therefore, the inlet condition of the channel flow is uniform velocity when the buoyancy parameter is small. One of the vertical side wall is heated uniformly and the opposite side wall is well insulated, as shown in Fig. 1(b). For the divergent channel, the insulated vertical plate is inclined with respect to the heated vertical plate so as to create a divergent angle of three degree with larger exit. The heated wall is made of 2 cm thick balsa wood and electrically heated. The uniform heating of the wall is achieved by gluing a number of 0.015 cm thick stainless steel foil strips on the entire side wall and passing an electric current through the foil heater. Therefore, the wall is given a uniform heat flux as the boundary condition. AC power is used to provide the electric energy for generating the desired heat flux. The heat flux can be determined by the electric voltage and current passing through the foil. The electric voltage drop due to the contact resistance between the heating strips and the terminals, which connect the heating strips with the AC power supply, has been taken into account. This kind of voltage drop is also noticed in other experiment [20]. For better insulation, a 12 cm thick foamed rubber is glued on the back of the heated wall. All the other side walls are wrapped with 5 cm thick foam rubber.

Since the temperature variation of the heated wall may be large in the vertical direction, the heated wall is instrumented with 12 rows of chromel–alumel thermocouples. One row of the thermocouples is along the mid-height of the wall. The distance between two neighboring rows is 2.5 cm, and the spacing between two neighboring thermocouples in each row is 1 cm. Therefore, there are a total of 22 thermocouples in each row. Since the surface temperature of the insulated wall is needed for estimating the radiation loss from the heated wall, five additional thermocouples are embedded along the surface of the wall. All thermocouples are calibrated in a constant temperature bath and the measurement error is found to be within  $\pm 0.1^\circ\text{C}$ . All the temperature signals are acquired with a FLUKE-2287A data logger connected to a computer for direct processing. The temperature data are taken when the entire system reaches steady state, usually in 3–4 hours.

During the flow visualization experiments, a smoke generator is used to supply smoke of fine particles, as shown in Fig. 1(a). The smoke particles are measured to be in a scale of  $2\ \mu\text{m}$  and are small enough to trace the flow in the channel. Smoke enters the channel from a slot of 1 mm width located on the surface in the immediate upstream of the channel entrance, as shown in Fig. 1(b). A vertical sheet of light perpendicular to the side insulated wall is used to visualize the circulation structure of secondary flow, while the sheet of light from the end parallel to the flow passage is used to visualize the flow structure from the side view. The flow patterns at the upstream, the central and the downstream regions can be observed and recorded.

The smoke particles injected were found to have no obvious effect on the heat transfer after rerunning the heat transfer measurements. During the experiments, the flow structure in the channel is sensitive to the circulation of ambient flow. Therefore, a windshield is constructed around the exit of the channel

to prevent this possible extraneous effect. The wind tunnel is similar to the one used in the studies of mixed convection in a heated vertical convergent or divergent channel [2,3] and [15–17] except that the insulated wall used here is not tilted, hence a detailed description is omitted here. The calibration needed for velocity measurement is also described in these reports. The total heat input in a single heating strip can be determined by the electric voltage and current passing through the strip. Since both conduction and radiation losses from each heating strip need to be accounted for and subtracted from the total energy supplied by the heater, the local heat transfer coefficient is evaluated by the following equation:

$$h_l = (q_r - q_{\text{rad}} - q_{\text{cond}})/(T_w - T_o) \quad (1)$$

where  $T_w$  is the local temperature on the heating strip, and  $T_o$  refers to the temperature at the inlet condition. The conduction loss from the heated wall is estimated by a one-dimensional conduction equation in a composite wall. The procedure to calculate the radiation loss from the heated wall is very similar to the one described in [20] and will not be repeated here. The thermophysical properties used in the local Nusselt number are evaluated at the bulk mean temperature of the flow, while those in the Reynolds and Grashof numbers are evaluated at the inlet temperature.

Since the channel flow exits directly to the ambient, the heat loss is relatively large near the exit. Therefore, the last three heating strips are used only as guard heaters. Relatively large heat loss in the exit region is also found in other experiments [4,20]. The uncertainty of the experimental data is determined according to the procedure proposed by Kline and McClintock [21]. The maximum uncertainty of local Nusselt number is 5.6%, while that for the Reynolds and Grashof number are 6.2 and 7.8%, respectively.

### 3. Results and discussions

#### 3.1. Flow visualizations

The smoke exits from a vertical, narrow slot on the heated sidewall at the inlet of the channel, and enters smoothly into the channel forming a vertical thin sheet of smoke along the side wall. As the thin-sheet smoke is heated, it moves upward, due to the buoyancy force, until reaching the top wall of the channel. The heated flow is essentially accumulated in the upper region of the channel as it moves downstream, as shown in Fig. 2. The accumulated flow circulates slowly in the upper region of the channel and grows in size due to the continuous supply of the heated buoyant flow along the side wall. The streamwise velocity of the accumulated flow is much slower than the mainstream. This attributed to the heated buoyant flow along the side wall whose velocity in the streamwise direction is significantly reduced by the viscous drag on the wall. Therefore, one could expect a lower heat transfer inside the accumulated flow region than the outside. The accumulated flow is the smoke region shown in Fig. 2 in the upper right portion of the channel as the flow enters the channel from the left end. Since the accumulated flow is warmer than the mainstream below, it is thermally stable. Therefore, the mainstream below will not break

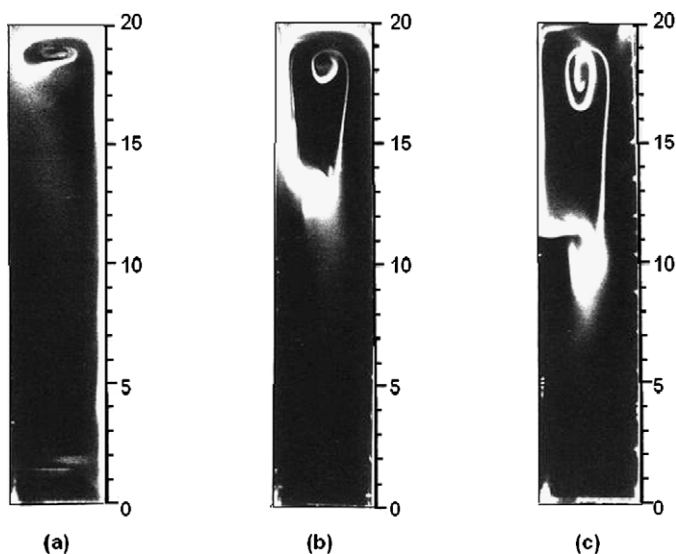


Fig. 2. Flow structure from the end view with  $Re = 700$  and  $Gr/Re^2 = 4000$  at (a)  $x = 10$  cm, (b)  $x = 25$  cm, and (c)  $x = 35$  cm.

into the accumulated flow region, mix with it and carry away even small portion of the accumulated flow. Therefore, the accumulated flow maintains at very stable condition and does not vary in size or location with time. As the buoyancy parameter increases, the accumulated flow region is initiated earlier and become larger in size, as shown in Fig. 3(a)–(c). At the extreme condition, e.g.,  $Gr/Re^2 = 7700$  as shown in Figs. 3(d) and 4, the heated buoyant flow starts accumulating at the entrance and the accumulated flow region has the largest size in the transverse direction. Even at this condition, the accumulated flow is still very stable. One can expect a reduction in the heat transfer enhancement by the buoyancy force in the region covered by the accumulated flow.

For the case of the divergent channel without the effect of buoyancy force, the mainstream decelerates due to enlargement of the cross section area of the channel as the flow moves downstream. The deceleration can cause destabilization of flow and lead to earlier transition into turbulent flow in a divergent channel [14]. For the case with the effect of buoyancy force, the destabilization can cause earlier initiation of the buoyancy induced flow [14,17,19]. This is expected to cause a greater enhancement of the heat transfer in the divergent channel as those divergent channels observed in other orientation [14,17, 19]. However, the buoyancy induced flow can accumulate in the upper region of the channel, and the accumulation can extend further upstream for the divergent channel than for the parallel plate channel as one compares the results in Fig. 3 with the ones in Fig. 4. For the case of  $Gr/Re^2$  greater than 6000, much of the buoyancy induced flow accumulated in the upper region of the channel has extended up to the entrance of the channel. Since the buoyancy induced flow accumulated in the upper region of the divergent channel covers a wider region of area than the case of the parallel plate channel, the reduction in the heat transfer enhancement by the buoyancy induced flow is larger in the divergent channel than in the parallel plate channel. However, the reduction in the heat transfer enhancement may not be so signif-

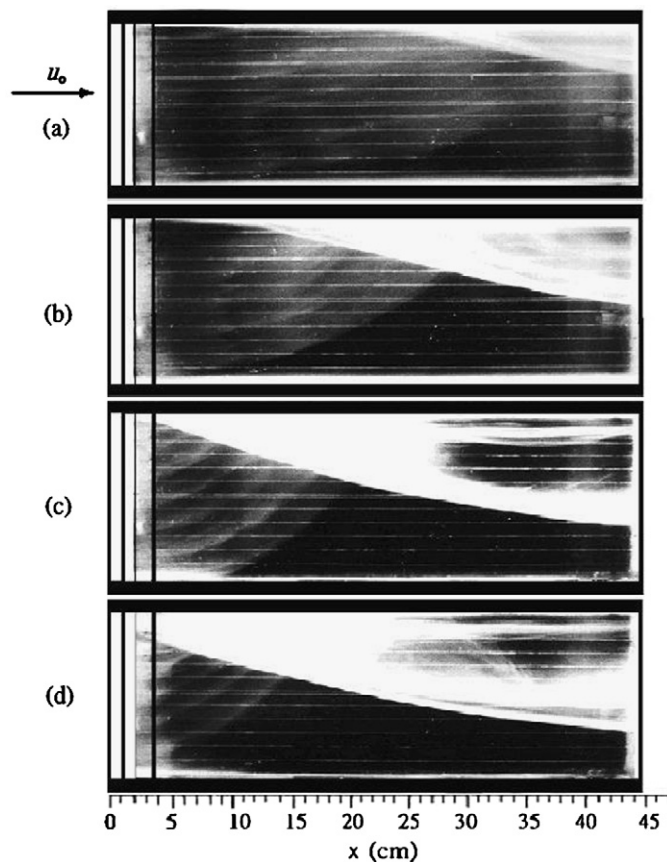


Fig. 3. Flow structure from the side view with  $Re = 500$  and  $Gr/Re^2 =$  (a) 1000, (b) 2000, (c) 6000, and (d) 7700 (for the parallel plate duct).

icant due to increase in the heat transfer by the earlier initiation of the buoyancy induced flow as a result of destabilization effect. Further discussion is presented in the next section of heat transfer measurements.

As the Reynolds number increases by increasing the flow velocity, one may expect that the entire accumulated flow region shifts downstream which leads to shrink in size. This may lead to the increase in the overall heat transfer enhancement by the buoyancy force. The downstream motion of the heated buoyant flow for mixed convection in a heated vertical channel indeed occurs as the Reynolds number increases and leads to reduction in the heat transfer enhancement by the buoyancy force [2, 3]. In the current experiments, however, previous expectation is not true if the buoyancy parameter  $Gr/Re^2$  is kept constant. As shown in Fig. 5, the entire accumulated flow region does not alter in size, shape and location when the buoyancy parameter is kept constant but the Reynolds number increases. This is attributed to the fact that by keeping  $Gr/Re^2$  constant the increase in the Reynolds number is counter-balanced by the increase in Grashof number, i.e., the increase in the inertia force in the streamwise direction is counter-balanced by the increase in the buoyancy force in the transverse direction. This leads to a result that the entire accumulated flow region stays in the same shape and position as long as the buoyancy parameter is maintained constant. That means that the enhancement in the over

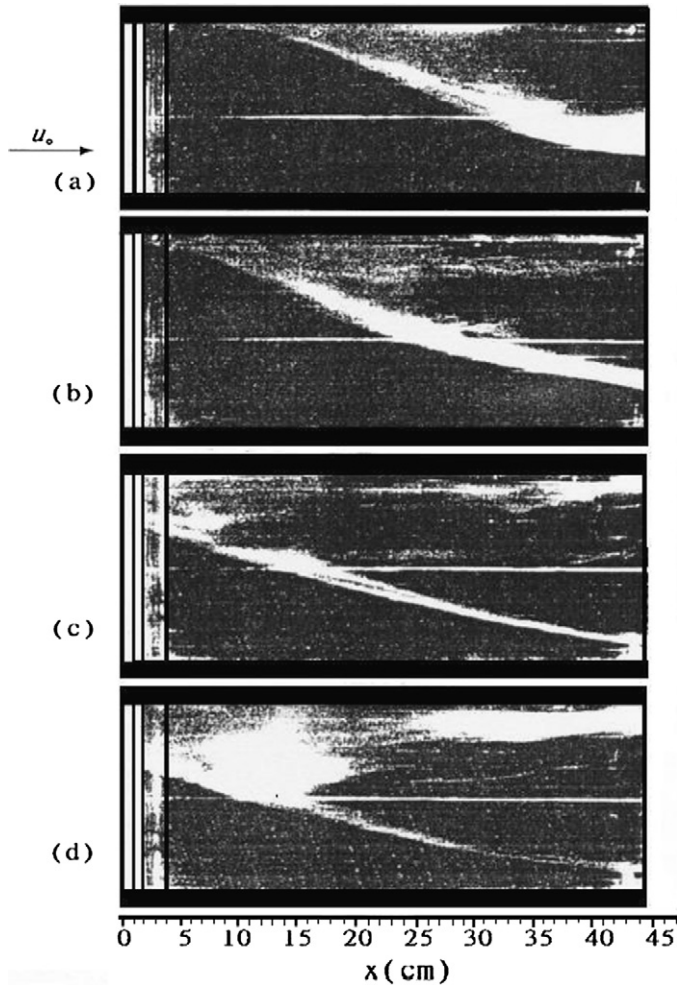


Fig. 4. Flow structure from the side view with  $Re = 500$  and  $Gr/Re^2 =$  (a) 1000, (b) 2000, (c) 6000, and (d) 7700 (for the divergent duct).

all heat transfer by the buoyancy force will remain the same if the buoyancy parameter is kept constant.

Similar kind of variation of flow structure with the buoyancy parameter  $Gr/Re^2$  is also found in divergent channel. The entire accumulated flow region shifts downstream, which leads to shrink in size as the buoyancy parameter reduces. However, the buoyancy induced flow accumulated in the upper portion of the channel extends over a wider region of area for the divergent channel than for the parallel plate channel.

### 3.2. Mixed convection heat transfer

To validate the heat transfer data measured, the Nusselt numbers for pure forced convection in the current channel are measured and compared with the data published in the literature. The agreement was found to be good. This gives us the confidence on the heat transfer data for the case of mixed convection. The entire distributions of the Nusselt numbers along the heated sidewall are shown in Fig. 6 for the parallel plate and the divergent channel. The contours of the Nusselt number are obtained by calculation from the local Nusselt number data at various locations. The Nusselt numbers vary along not only the streamwise direction but also the transverse direction. The vari-

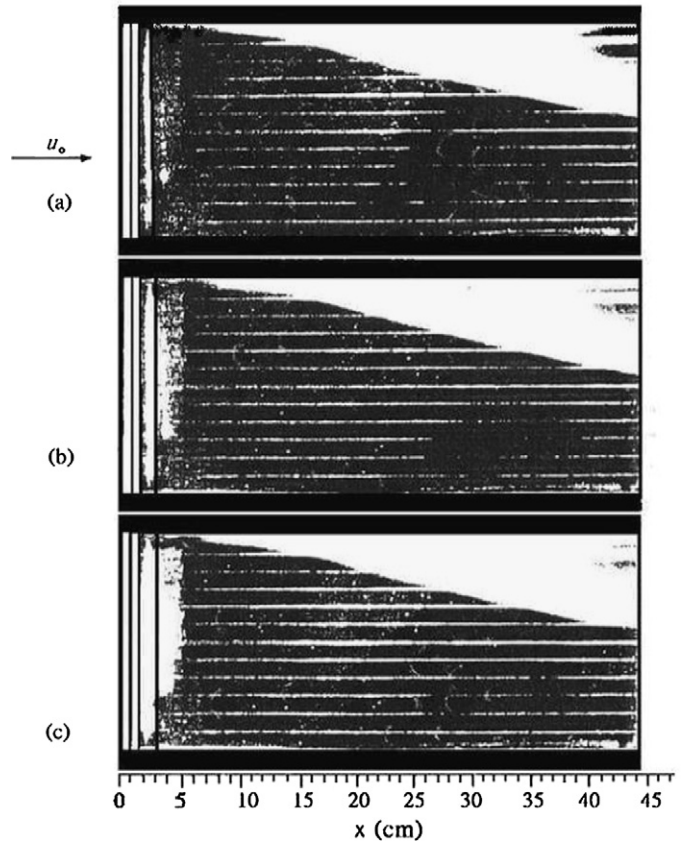


Fig. 5. Flow structure from the side view with  $Gr/Re^2 = 2000$ ; (a)  $Re = 500$ , (b)  $Re = 700$ , and (c)  $Re = 1000$ .

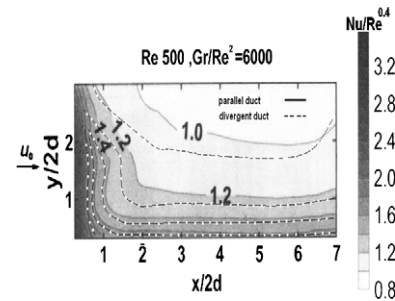


Fig. 6. The normalized Nusselt number contours on the heated side wall with  $Gr/Re^2 = 6000$  and  $Re = 500$ .

ation in the transverse direction is attributed only to the free convection effect which makes the heat transfer in the lower region of the channel higher than the upper region. The variation in the streamwise direction is attributed to the combined free and forced convection. By carefully examining the heat transfer data in the accumulated flow region and the region outside, one found that the heat transfer in the accumulated flow region is essentially lower, as expected, due to the lower velocity of the flow in both the transverse and the streamwise direction. In addition, the heat transfer in the accumulated flow region in the divergent channel is much lower than in the parallel plate channel due to a wider region of accumulated flow in the divergent channel. However, in the region outside the accumulated flow

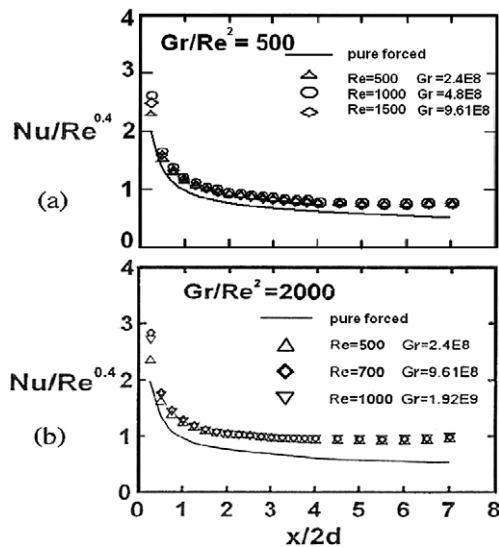


Fig. 7. The normalized Nusselt number distributions for the parallel plate duct at different Reynolds numbers with (a)  $Gr/Re^2 = 500$  and (b)  $Gr/Re^2 = 2000$ .

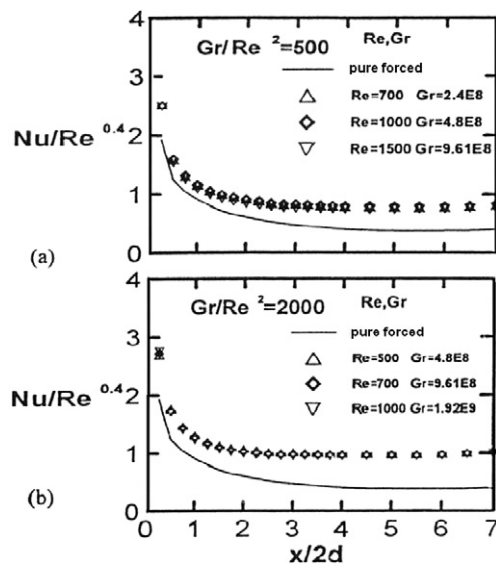


Fig. 8. The normalized Nusselt number distributions for the divergent duct at different Reynolds numbers with (a)  $Gr/Re^2 = 500$  and (b)  $Gr/Re^2 = 2000$ .

the heat transfer for the divergent channel approaches for the parallel plate channel.

At a given streamwise location, the Nusselt numbers at different heights differ due to the effect of the free convection and the accumulated flow. It appears that the Nusselt number distribution in the transverse direction can be averaged which represents the mixed convection heat transfer with an averaged effect of free convection or the buoyancy force in the transverse direction. To simplify the presentation and the analysis, therefore, the Nusselt number distributions are averaged in the transverse direction. The averaged Nusselt numbers are then plotted along the streamwise direction at different buoyancy parameters and compared with parallel and divergent duct. In this way, one can readily study the effect of buoyancy parameter and

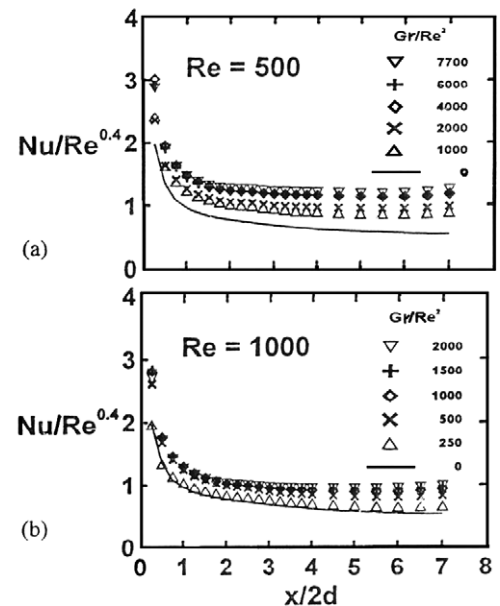


Fig. 9. The normalized Nusselt number distributions at different buoyancy parameter in parallel duct with (a)  $Re = 500$  and (b)  $Re = 1000$ .

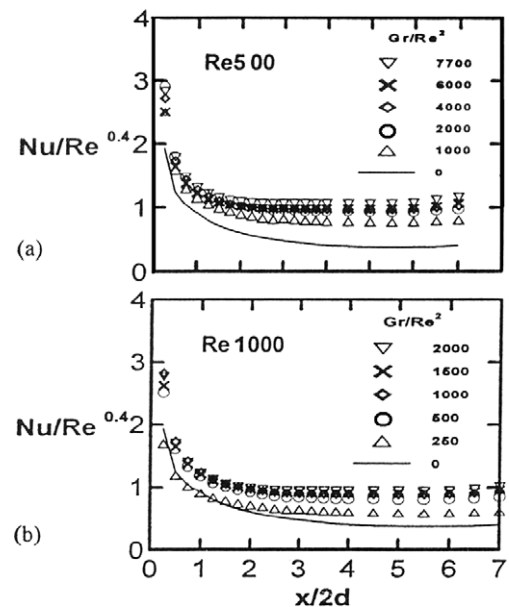


Fig. 10. The normalized Nusselt number distributions at different buoyancy parameter for the divergent duct with (a)  $Re = 500$  and (b)  $Re = 1000$ .

geometry on the heat transfer inside the duct in a clear fashion. Therefore, Figs. 7–13 are presented in this way.

For pure forced convection, Gau [3] found that the normalized Nusselt number at different Reynolds number can collapse into a single line if the Nusselt number is defined based on the air temperature at the inlet of the channel and is normalized by  $Re^{0.4}$ . By plotting the heat transfer data in this way, the Reynolds number effect can be eliminated. This is useful to study buoyancy effect on the heat transfer in a duct with mixed convection occurring inside. For mixed convection in a heated vertical channel, Gau [2] found that the normalized Nusselt numbers indeed could collapse into a single line in certain

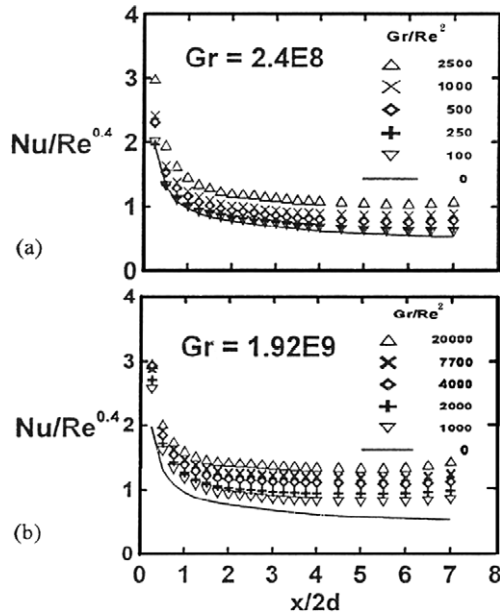


Fig. 11. The normalized Nusselt number distributions at different buoyancy parameter by changing the Reynolds numbers with (a)  $Gr = 2.4 \times 10^8$  and (b)  $Gr = 1.92 \times 10^9$ .

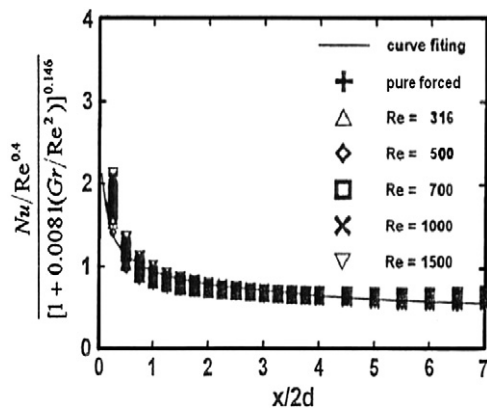


Fig. 12. Correlation of the normalized Nusselt numbers for the parallel duct in terms of the buoyancy parameter.

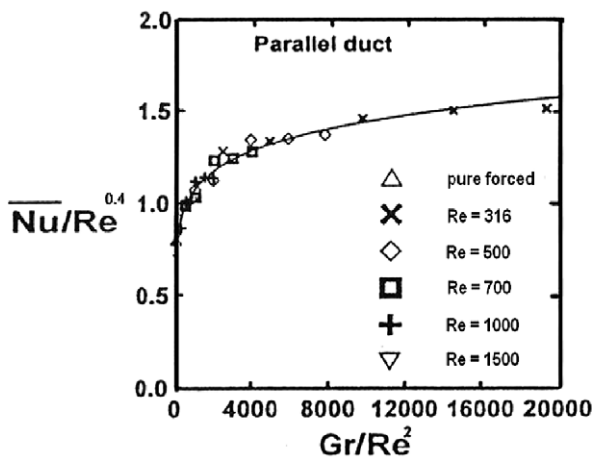


Fig. 13. Correlation of the average in the normalized Nusselt numbers in terms of the buoyancy parameter (over the entire parallel plate duct).

regions of the buoyancy parameters when  $Gr/Re^2$  is kept constant. That is the case when the buoyant heated, reversed flow has not been initiated; or the case when the buoyant heated, reversed flow has occurred and spread over the entire duct. When the buoyancy parameters  $Gr/Re^2$  are not so large that the buoyant heated, reversed flow is initiated only in certain region of the duct, then the normalized Nusselt numbers do not collapse into a single line. This was attributed to the fact that the buoyant heated, reversed flow is significantly affected by the changes of the Reynolds number as  $Gr/Re^2$  is kept constant. However, the previous flow visualization clearly indicates that the accumulated flow region due to the buoyant heated flow is not affected at all by the Reynolds number if the buoyancy parameter is kept constant. One thus plots the normalized Nusselt number results, as shown in Fig. 7 (a) and (b) for the parallel plate channel, and Fig. 8 (a) and (b) for the divergent channel, under the same buoyancy parameter but different Reynolds numbers. It appears that all the normalized Nusselt numbers at different Reynolds numbers collapse into a single line when  $Gr/Re^2$  is kept constant. In the following presentation, therefore, one can study the buoyancy effect on the heat transfer.

The variation of the buoyancy parameter can be done by changing either the values of  $Gr$  or the values of  $Re$  during the experiments. Figs. 9–11 show that the normalized Nusselt numbers increase with increasing the buoyancy parameters. This is true within the ranges of current experimental conditions. In Figs. 9–11, the increase of the buoyancy parameter is done by increasing the value of  $Gr$ . However, in Fig. 11 the increase of the buoyancy parameter is done by decreasing the value of  $Re$ . It appears that  $Gr/Re^2$  is the only dimensionless parameter to affect the heat transfer enhancement as a result from the buoyancy force. As long as the value of  $Gr/Re^2$  is kept constant, the enhancement in the heat transfer by the buoyancy force is the same.

Comparing the normalized Nusselt numbers for the case of the parallel plate channel and the case of the divergent channel, as shown in Figs. 9 and 10, the normalized Nusselt number under the buoyancy force effect is very close for both channels. For the pure forced convection, however, the normalized Nusselt number in the divergent channel is lower than in the parallel plate channel due to divergence of the channel which can decrease the velocity of the flow. However, due to the destabilization effect, initiation of the buoyancy induced flow in the divergent channel can be easier and earlier. This may cause greater enhancement in the heat transfer than in the parallel plate channel. However, the accumulated flow due to buoyant, heated flow in the divergent channel can be extended over a wider region. This can have an opposite effect to reduce the heat transfer. The counter effect of enhancement and reduction in the heat transfer in the divergent channel makes the heat transfer almost identical to the one in parallel plate channel. The current experimental results indicate that slight inclination of the side wall of the channel does not have a significant effect on the heat transfer when buoyancy induced flow occurs. This finding appears to oppose the one for mixing convection in ver-

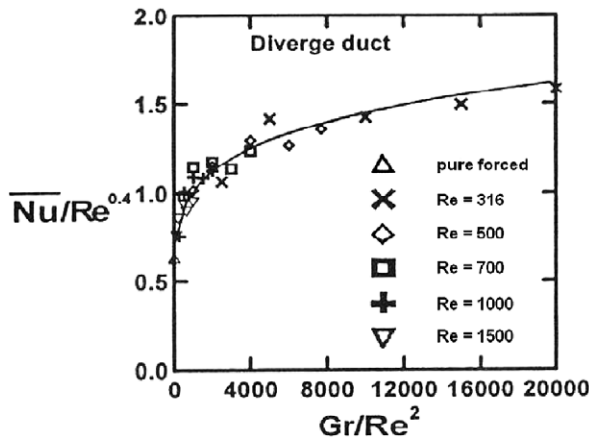


Fig. 14. Correlation of the average in the normalized Nusselt numbers in terms of the buoyancy parameter (over the entire divergent duct).

tical channel heating on one side [15–17] or horizontal channel heated from below [14,18,19] where slight inclination of the insulated side wall of the channel can have a significant effect on both the flow and the heat transfer.

The above results indicate that keeping the buoyancy parameter constant, the variation of the Reynolds number does not have any effect on the size, shape and location of the accumulated flow. This suggests that the buoyant heated flow and the heat transfer data can be properly correlated in terms of the buoyancy parameter. The Reynolds number effect on the heat transfer can be eliminated by dividing the Nusselt number defined in the current report by  $Re^{0.4}$ . The increase of the buoyancy parameter either by increasing  $Gr$  or decreasing  $Re$  will identically lead to an increase in the normalized Nusselt number. The increase in the normalized Nusselt numbers is in proportion to the buoyancy parameter. Correlations of both the local (averaged in the transverse direction) and the averaged (over the entire duct) Nusselt number in terms of the buoyancy parameter are performed, and the results are shown in Figs. 12 and 13.

For correlation of the local Nusselt number in terms of the buoyancy parameter,

$$\frac{Nu}{Re^{0.4}} = \frac{0.94 \times [1 + 0.0081(Gr/Re^2)]^{0.146}}{(x/2d)^{0.272}} \quad (2)$$

which has a standard deviation of 0.042.

And the average Nusselt number correlated for the parallel duct in terms of the buoyancy parameter is obtained as follows:

$$\frac{\bar{Nu}}{Re^{0.4}} = 0.83 \times [1 + 0.0081(Gr/Re^2)]^{0.126} \quad (3)$$

which has a standard deviation of 0.011.

Both Eqs. (2) and (3) are valid for the Reynolds number in the range from 316 to 1500 and the buoyancy parameter  $Gr/Re^2$  is from 100 to 20000.

The Nusselt results for the divergent channel are very similar to the results for the parallel plate channel, as shown in Fig. 14 for the correlation of the averaged Nusselt number in the divergent channel. Both Eqs. (2) and (3) can also be used

for divergent channel with accuracy of less than 5% difference from the divergent channel.

#### 4. Conclusions

Effect on channel divergence on the mixed convection flow and the heat transfer process in a divergent duct heated from a side are studied experimentally. For comparison, the mixed convection in the parallel plate channel is also studied and presented. Due to the vertical buoyancy force, the heated buoyant flow moves upward and accumulated in the upper region of the duct. The accumulated flow is thermally stable which grows in size as the buoyancy parameter increases. The effect of slight inclination of the side wall can significantly increase the amount and the area of the accumulated flow region, which can significantly reduce the heat transfer. In addition, the deceleration of the channel flow can also reduce the heat transfer in the divergent channel. However, the destabilization effect of the divergent channel has an opposite effect to increase the heat transfer. These counter effects of increasing and reducing the heat transfer process makes the heat transfer in the divergent channel almost identical to the one in the parallel plate channel. This finding is oppose to the one for mixing convection in channels with different orientations where slight inclination of the side wall can have a significant effect on both the flow and the heat transfer. Correlations for the normalized Nusselt number in terms of buoyancy parameter in the parallel plate channel are obtained, which can also be used with sufficient accuracy in the divergent channel having slight inclination of the side wall.

#### References

- [1] W. Aung, G. Worku, Developing flow and flow reversal in a vertical channel with asymmetric wall temperatures, *ASME J. Heat Transfer* 108 (1986) 299–304.
- [2] C. Gau, K.A. Yih, W. Aung, Reverse flow structure and heat transfer measurements for buoyancy-assisted convection in heated vertical duct, *ASME J. Heat Transfer* 114 (1992) 928–935.
- [3] C. Gau, K.A. Yih, W. Aung, Measurements of heat transfer and flow structure in heated vertical channels with buoyancy assisted and opposed flows, *AIAA J. Thermophys. Heat Transfer* 6 (4) (1992) 707–712.
- [4] R.A. Wirtz, P. McKinley, Buoyancy effects on downward laminar convection between parallel-plates, in: *Fundamentals of Forced and Mixed Convection*, ASME HTD, vol. 42, 1985, pp. 105–112.
- [5] G.J. Hwang, C.L. Liu, An experimental study of convective instability in the thermal entrance region of a horizontal parallel-plate channel heated from below, *Can. J. Chem. Engng.* 54 (1976) 521–525.
- [6] F.P. Incropera, A.L. Knox, J.R. Maughan, Mixed convection flow and heat transfer in the entry region of a horizontal rectangular duct, *ASME J. Heat Transfer* 109 (1987) 434–439.
- [7] H.V. Mahaney, F.P. Incropera, S. Ramadhyani, Development of laminar mixed convection in the thermal entrance region of horizontal rectangular ducts, *Numer. Heat Transfer* 12 (1987) 137–155.
- [8] J.R. Maughan, F.P. Incropera, Regions of heat transfer enhancement for laminar mixed convection in a parallel plate channel, *Int. J. Heat Mass Transfer* 33 (1990) 555–570.
- [9] F.S. Lee, G.J. Hwang, The effect of asymmetric heating on the onset of thermal instability in the thermal entrance region of a parallel-plate channel, *Int. J. Heat Mass Transfer* 34 (1991) 2207–2218.
- [10] W. Aung, Mixed convection in internal flow, in: S. Kakac, R.K. Shah, W. Aung (Eds.), *Handbook of Single Phase-phase Convective Heat Transfer*, Wiley, New York, 1987 (Chapter 15).



- [11] C. Gau, Y.C. Jeng, C.G. Liu, An experimental study of mixed convection in a horizontal channel heated from a side, *ASME J. Heat Transfer* 122 (4) (2000) 701–707.
- [12] M.E. Ali, Natural convection heat transfer from horizontal rectangular ducts, *J. Heat Transfer* 129 (9) (2007) 1195–1202.
- [13] M.S. Hatamipour, D. Mowla, Experimental investigation of heat transfer in an air duct with an inclined heating surface, *Chem. Engng. Comm.* 190 (4) (2003) 508–518.
- [14] C. Gau, T.M. Huang, C.W. Liu, W. Aung, Mixed convection flow and heat transfer in a horizontal divergent channel with bottom wall heated, in: *Proceedings of the 11th International Heat Transfer Conference*, vol. 3, Kyongju, Korea, Aug. 23–28, 1998, pp. 257–262.
- [15] C. Gau, T.M. Huang, W. Aung, Mixed convection flow and heat transfer in a heated vertical convergent channel, *Internat. J. Heat Mass Transfer* 38 (13) (1995) 2445–2456.
- [16] T.M. Huang, C. Gau, W. Aung, Mixed convection flow and heat transfer in a vertical convergent channel, *Internat. J. Heat Mass Transfer* 38 (13) (1995) 2445–2456.
- [17] T.M. Huang, C. Gau, W. Aung, Flow and mixed convection heat transfer in a divergent heated vertical channel, *ASME J. Heat Transfer* 118 (3) (1996) 606–615.
- [18] C. Gau, C.W. Liu, T.M. Huang, W. Aung, Secondary flow and enhancement of heat transfer in horizontal parallel-plate and convergent channels heating from below, *Internat. J. Heat Mass Transfer* 42 (1999) 2629–2647.
- [19] C.W. Liu, C. Gau, Onset of secondary flow and enhancement of heat transfer in horizontal convergent and divergent channels heated from below, *Internat. J. Heat Mass Transfer* 47 (2004) 5427–5438.
- [20] B.W. Webb, D.P. Hill, High Rayleigh number laminar natural convection in a symmetrically heated vertical channel, *ASME J. Heat Transfer* 111 (1989) 649–656.
- [21] S.J. Kline, F.A. McClintock, Describing uncertainties in single-sample experiments, *Mech. Engng.* 75 (1953) 3–12.